Letter

Search for diphoton decays of an axionlike particle in radiative J/ψ decays

M. Ablikim *et al.*[*]
(BESIII Collaboration)

(Received 10 April 2024; accepted 2 July 2024; published 6 August 2024)

We search for the diphoton decay of a light pseudoscalar axionlike particle, a, in radiative J/ψ decays, using 10^{10} J/ψ events collected with the BESIII detector. We find no evidence of a signal and set upper limits at the 95% confidence level on the product branching fraction $\mathcal{B}(J/\psi \to \gamma a) \times \mathcal{B}(a \to \gamma\gamma)$ and the axionlike particle photon coupling constant $g_{a\gamma\gamma}$ in the ranges of $(3.7\text{–}48.5) \times 10^{-8}$ and $(2.2\text{–}101.8) \times 10^{-4}\ \mathrm{GeV}^{-1}$, respectively, for $0.18 \leq m_a \leq 2.85\ \mathrm{GeV}/c^2$. These are the most stringent limits to date in this mass region.

DOI: 10.1103/PhysRevD.110.L031101

Axions are hypothetical pseudoscalar gauge bosons originally proposed by Peccei and Quinn as a mechanism of spontaneous U(1) symmetry breaking to resolve the strong CP problem in quantum chromodynamics [1–3] and later applied to the electroweak hierarchy problem [4]. Axionlike particles (ALPs) have the same quantum numbers as the QCD axion, but they have different masses and couplings. ALPs appear in various extensions of the Standard Model (SM), such as supersymmetry [5–7], extended Higgs sector [8], and string theory [9–12]. The ALPs can act as a mediator between the dark sector and ordinary matter [13,14], and they could be cold dark matter candidates in certain situations [15–18]. A light scalar decaying to two photons could also be a signature of a CP-violating minimal supersymmetric Standard Model [19] or Fermi-phobic Higgs bosons [20]. Experimental constraints on these scenarios are important to understanding the properties of the SM Higgs boson [21]. In a simple scenario, the ALP, a, predominantly couples to a photon pair with a coupling constant $g_{a\gamma\gamma}$. Reference [22] has recently discussed the phenomenology of gravitonlike spin-2 particles and the reinterpretation of existing experimental bounds on $g_{a\gamma\gamma}$ to set bounds on these possibilities.

Experimental bounds on $g_{a\gamma\gamma}$ for masses of a in the sub-MeV$/c^2$ range are available from laser experiments, solar photon instruments, and astrophysical observations [23,24], while the experimental bounds on the photon coupling in the MeV$/c^2$–GeV$/c^2$ range mainly come from beam-dump and high-energy collider experiments [25–27].

Limits on long-lived ALPs are derived from radiative decays $V \to \gamma + \text{invisible}$ $[V = \Upsilon(1S), J/\psi]$ [28,29] and the $e^+e^- \to \gamma + \text{invisible}$ reaction [30–33]. On the other hand, short-lived ALPs decaying to a photon pair are searched for in $e^+e^- \to \gamma\gamma(\gamma)$ reactions [34–36], the light-by-light scattering process $\gamma\gamma \to \gamma\gamma$ [37,38], pp collisions [39–41], and radiative $J/\psi \to \gamma a$ decays, based on 2.7×10^9 $\psi(3686)$ events at BESIII [42]. The previous BESIII measurement [42] selected a sample of approximately 10^9 J/ψ events by tagging the pion pair from the $\psi(3686) \to \pi^+\pi^- J/\psi$ transition. The ALP-photon coupling in the ALP mass range of $(0.1\text{–}5)\ \mathrm{GeV}/c^2$ is less constrained than the other mass regions. The best upper bound on $g_{a\gamma\gamma}$ mainly comes from the previous BESIII measurement [42] for $0.165 \leq m_a \leq 1.468\ \mathrm{GeV}/c^2$ and OPAL [34] measurement in the rest of the mass region. The large data sample collected by the BESIII detector at the J/ψ resonance [43] can further improve the sensitivity on $g_{a\gamma\gamma}$ in the mass region $0.18 \leq m_a \leq 2.85\ \mathrm{GeV}/c^2$ [44].

In J/ψ decays, ALP production predominantly proceeds via the radiative decay $J/\psi \to \gamma a$ [45]. The branching fraction of $J/\psi \to \gamma a$ relates to $g_{a\gamma\gamma}$ as [45]

$$\frac{\mathcal{B}(J/\psi \to \gamma a)}{\mathcal{B}(J/\psi \to e^+e^-)} = \frac{m_{J/\psi}^2}{32\pi\alpha} g_{a\gamma\gamma}^2 \left(1 - \frac{m_a^2}{m_{J/\psi}^2}\right)^3, \qquad (1)$$

where α is the fine-structure constant, m_a is the mass of the ALP, and $m_{J/\psi}$ is the mass of the J/ψ meson. Additional processes contributing to the same final state are the ALP-strahlung $e^+e^- \to \gamma a$ process [45] and the radiative production of pseudoscalar mesons through $J/\psi \to \gamma P$ with $P = \{\pi^0, \eta, \eta', \eta_c\}$ [46,47].

This article describes the search for a light pseudoscalar ALP in radiative decays of the J/ψ using $(1.0087 \pm 0.0044) \times 10^{10}$ J/ψ events collected with the BESIII detector [43]. This search assumes that the direct coupling

[*]Full author list given at the end of the article.

of the ALP to charm quarks is negligible, and that the ALP produced in $J/\psi \to \gamma a$ couples to the virtual photon created in $c\bar{c}$ annihilation [45]. Since the ALP-strahlung process $e^+e^- \to \gamma a$ is indistinguishable from ALP production in radiative J/ψ decays in the case of a null result, the expected 4.4% ALP-strahlung contribution [45] is subtracted from the experimental measurement to derive constraints on the $J/\psi \to \gamma a$ branching ratio. The interference between the ALP-strahlung process $e^+e^- \to \gamma a$ and radiative $J/\psi \to \gamma a$ is predicted to be negligible due to the small J/ψ width [45].

The BESIII detector [48] records symmetric e^+e^- collisions provided by the BEPCII storage ring [49] in the center-of-mass energy range from 2.0 to 4.95 GeV with a peak luminosity of $1 \times 10^{33}\ \mathrm{cm}^{-2}\,\mathrm{s}^{-1}$ achieved at $\sqrt{s} = 3.77$ GeV. BESIII has collected large data samples in this energy region [50–52]. The cylindrical core of the BESIII detector covers 93% of the full solid angle and consists of a helium-based multilayer drift chamber, a plastic scintillator time-of-flight system (TOF), and a CsI (Tl) electromagnetic calorimeter (EMC), which are all enclosed in a superconducting solenoidal magnet providing a 1.0 T (0.9 T in 2012, for about 11% of the dataset) magnetic field. The solenoid is supported by an octagonal flux-return yoke with resistive plate counter muon identification modules interleaved with steel. The charged-particle momentum resolution at 1 GeV/c is 0.5%. The EMC measures photon energies with a resolution of 2.5% (5%) at 1 GeV in the barrel (end cap) region. The time resolution in the TOF barrel region is 68 ps, while that in the end cap region is 110 ps. The end cap TOF system was upgraded in 2015 using multigap resistive plate chamber technology, providing a time resolution of 60 ps. About 87% of the dataset benefits from this upgrade.

Monte Carlo (MC) simulated data samples produced with a GEANT4-based software package [53], which includes the geometrical acceptance of the detector and time-dependent beam related backgrounds, are used to optimize the event selection criteria, study the potential backgrounds, and evaluate the reconstruction efficiency. A MC sample of 10^{10} inclusive J/ψ decays is used for background studies with the TopoAna tool [54]. In this sample, the known decay modes of J/ψ are simulated by EVTGEN [55] with their branching fractions taken from the Particle Data Group (PDG) [46] and the remaining unknown decay modes by LUNDCHARM [56]. The production of the J/ψ resonance via e^+e^- annihilation, including beam energy spread and initial-state radiation (ISR), is simulated by KKMC [57]. The backgrounds from the SM processes $e^+e^- \to \gamma\gamma(\gamma)$ and $e^+e^- \to \gamma P$ are estimated with 166.3 pb^{-1} of continuum data collected at the center-of-mass energy of 3.08 GeV [43]. To evaluate the signal efficiency, simulated signal MC events are generated for 33 values of m_a ranging from 0.1 to 3.0 GeV/c^2 with a phase-space model for $a \to \gamma\gamma$ and a P-wave model for the $J/\psi \to \gamma a$ decay [55]. To avoid any bias, a semiblind procedure is adopted in which approximately 10% of the full J/ψ data is used to check the agreement between data and background predictions and validate the fitting approach. The rest of the J/ψ dataset is blinded until the analysis procedure is frozen.

We select the events of interest with at least three photon candidates and zero charged tracks in the final state. The photon candidates are reconstructed using the energy clusters deposited in the EMC barrel region with a minimum energy of 25 MeV. End cap clusters are not used in order to suppress the background from $e^+e^- \to \gamma\gamma(\gamma)$ events. The energy deposited in the nearby TOF scintillators is also included to improve the reconstruction efficiency and energy resolution. The EMC time difference between any two photons is required to be within the range of $-500 < \Delta T < 500$ ns to suppress electronics noise and energy deposits unrelated to the events. To improve the mass resolution, a four-constraint (4C) kinematic fit is performed, constraining the mass of the three-photon system to the center-of-mass energy. If there is more than one $J/\psi \to \gamma\gamma\gamma$ combination, the candidate with the minimum value of the χ^2 from the kinematic fit (χ^2_{4C}) is retained. The χ^2_{4C} is required to be less than 30. A similar 4C kinematic fit is also separately performed with all possible two-, four-, and five-photon candidate hypotheses. We require that the χ^2_{4C} of the three-photon candidate hypothesis is less than that for the other hypotheses to avoid any wrong combination of soft photons. The requirements of $\chi^2_{4C} < \chi^2_{4C}(2\gamma)$ and $\chi^2_{4C} < \chi^2_{4C}(n\gamma)$ ($n = 4, 5$) suppress the backgrounds from the $e^+e^- \to \gamma\gamma$ process and $J/\psi \to \gamma\pi^0\pi^0$ decays when a low-energy photon escapes undetected. The selected three photon candidates are used for further analysis.

In order to further suppress the $e^+e^- \to \gamma\gamma(\gamma)$ events with low-energy EMC clusters, the energy difference between the first (second) and third photon candidates, $\Delta E_{\gamma_{ij}}$, is required to be less than 1.46 (1.41) GeV, where the first, second, and third photons are sorted by decreasing energy. The absolute azimuthal angle difference between the third and first photon candidates, $\Delta\phi_{\gamma_{31}}$, is also required to be greater than 1 rad.

At this stage, the dominant background contributions come mainly from $J/\psi \to \gamma P$, where P denotes the pseudoscalar mesons $\pi^0, \eta, \eta', \eta_c$, as also seen in Refs. [42,47]. To validate the signal extraction procedure (see below) the same fit is used to extract the branching fractions of $J/\psi \to \gamma(\pi^0, \eta, \eta') \to \gamma\gamma\gamma$. After accounting for the peaking background contributions, such as $J/\psi \to \gamma\pi^0\pi^0$ in $J/\psi \to \gamma\pi^0$ decay as described in Ref. [47], the results are compatible with the measurements of Ref. [47] and PDG averages [46] within their uncertainties. We further reject the events where the diphoton invariant mass ($m_{\gamma\gamma}$) for any photon combination is in the regions

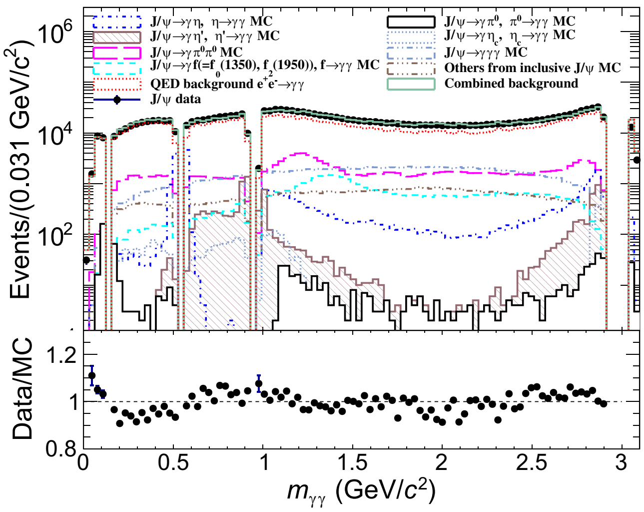

FIG. 1. Distribution of the diphoton invariant mass, $m_{\gamma\gamma}$, for data (black dots with error bars) together with the background predictions of the QED $e^+e^- \to \gamma\gamma$ process from data collected at 3.08 GeV (dotted red curve), $J/\psi \to \gamma\pi^0\pi^0$ (long-dashed pink curve), $J/\psi \to \gamma\gamma\gamma$ (double-dotted long-dashed gray curve), $J/\psi \to \gamma f$ $[f = f_0(1350), f_2(1950)]$ (long-dashed cyan curve), $J/\psi \to \gamma P$ (brown pattern, dashed-dotted blue, black and dotted gray histograms), and other backgrounds from inclusive J/ψ decays (triple-dotted long-dashed brown curve). The solid green olive histogram represents the combined background. The bottom panel shows the ratio of data to the combined background predictions.

$0.11 \le m_{\gamma\gamma} \le 0.16$ GeV$/c^2$, $0.52 \le m_{\gamma\gamma} \le 0.56$ GeV$/c^2$, $0.92 \le m_{\gamma\gamma} \le 0.99$ GeV$/c^2$, and $2.92 \le m_{\gamma\gamma} \le 3.04$ GeV$/c^2$ to suppress the backgrounds from $J/\psi \to \gamma\pi^0$, $J/\psi \to \gamma\eta$, $J/\psi \to \gamma\eta'$, and $J/\psi \to \gamma\eta_c$, respectively.

After applying the above selection criteria, the signal yields are extracted from the data by performing a series of one-dimensional unbinned extended maximum likelihood (ML) fit to the $m_{\gamma\gamma}$ distribution, which includes all combinations of two photon pairs. The fit function includes the contributions of signal and backgrounds and is described in more detail below.

Figure 1 shows the $m_{\gamma\gamma}$ distribution for data and various background predictions. The dominant background comes from the QED process $e^+e^- \to \gamma\gamma(\gamma)$, which is predicted from the continuum data collected at 3.08 GeV. The $m_{\gamma\gamma}$ distribution for data is generally well described by the background predictions, except in the low-mass region, where KKMC [57] fails to reproduce the events for J/ψ decaying to multiphotons in the final state. This disagreement has a minor impact on the ALP search because the signal extraction procedure does not depend on the predictions of the background yields. In order to mitigate the effect from the tails of the peaking backgrounds $J/\psi \to \gamma P$, the fit is performed in different $m_{\gamma\gamma}$ intervals for various m_a points, as described in Table I.

TABLE I. The fit intervals of $m_{\gamma\gamma}$ for various m_a points.

m_a range (GeV$/c^2$)	$m_{\gamma\gamma}$ fit interval (GeV$/c^2$)	Polynomial function order
0.180–0.420	0.16, 0.46	Fourth
0.421–0.490	0.39, 0.51	Fifth
0.610–0.880	0.59, 0.90	Fifth
1.020–1.099	1.00, 1.20	Fifth
1.100–2.770	$m_a - 0.10$, $m_a + 0.10$	Third
2.772–2.850	2.70, 2.88	Fourth

Simulated data samples are used to construct the signal and background probability density functions (PDFs). The signal PDF is described by the sum of two crystal ball functions with common mean and opposite-side tails. The efficiency and parameters of the crystal ball functions are obtained from the simulated signal MC samples by performing a fit to the $m_{\gamma\gamma}$ distribution. This fit includes the contributions of signal and combinatorial background from wrong $\gamma\gamma$ combinations, described by a first-order Chebyshev function. The m_a resolution varies from 6 to 15 MeV$/c^2$ while the signal selection efficiency, ϵ, varies from 28.2% to 39.0% depending on the a mass. The PDF parameters and efficiency of the signal are interpolated linearly between the mass points of the generated signal MC samples. The background PDF is described by third-, fourth-, and fifth-order Chebyshev functions in various $m_{\gamma\gamma}$ fit regions detailed in Table I.

The search is performed in 1.0 MeV$/c^2$ steps in the mass range of $0.18 \le m_a \le 1.5$ GeV$/c^2$ and 2.0 MeV$/c^2$ steps for higher m_a values. The free parameters of the fit are the number of signal events ($N_{\rm sig}^{\rm dat}$), which includes the contributions of both radiative $J/\psi \to \gamma a$ and ALP-strahlung $e^+e^- \to \gamma a$ process, the number of background events, and the shape parameters of the background PDF. To take into account a possible systematic uncertainty associated with the choice of PDFs, the fit is repeated with an alternative signal PDF described by a Cruijff function [58], or increasing by one the order of the Chebyshev polynomial function for the background PDF at each m_a point. The fit with the largest signal yield, giving the worst upper limit, is chosen to produce the final result. The final signal yield $N_{\rm sig}$ is 95.6% of the $N_{\rm sig}^{\rm dat}$ after subtracting the contribution from the ALP-strahlung process [45].

We calculate the product branching fraction of $J/\psi \to \gamma a$ and $a \to \gamma\gamma$ at each m_a point using the following formula,

$$\mathcal{B}(J/\psi \to \gamma a) \times \mathcal{B}(a \to \gamma\gamma) = \frac{N_{\rm sig}}{\epsilon N_{J/\psi}}. \quad (2)$$

Figure 2 shows the product branching fraction $\mathcal{B}(J/\psi \to \gamma a) \times \mathcal{B}(a \to \gamma\gamma)$ and the statistical significance, defined as $\mathcal{S} = \sqrt{-2\ln(\mathcal{L}_0/\mathcal{L}_{\rm max})}$, as a function of m_a. In this

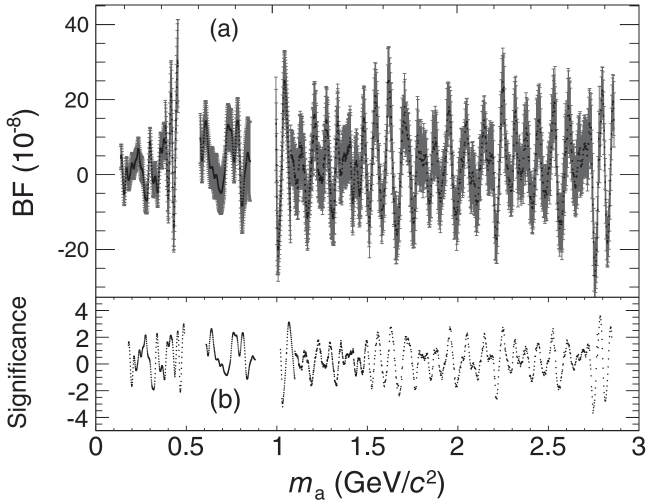

FIG. 2. (a) Product branching fraction $\mathcal{B}(J/\psi \to \gamma a) \times \mathcal{B}(a \to \gamma\gamma)$ (BF) and (b) the signal significance versus m_a obtained from the fit, as described in the text.

formula $\mathcal{L}_{\max}$ and $\mathcal{L}_0$ are the likelihood functions for the number of signal events obtained from the fit and fixed at zero, respectively. The largest value of upward local significance is determined to be 3.5σ at $m_a = 2.786$ GeV$/c^2$. The fit result for the corresponding m_a point is shown in Fig. 3. We estimate the probability of observing a fluctuation of $\mathcal{S} \geq 3.5\sigma$ to be 5.2% using a large ensemble of pseudoexperiments [59]. The corresponding global significance value is 1.6σ. Thus, we conclude that no significant evidence of signal events is found within the investigated m_a regions.

As follows from Eqs. (1) and (2), the systematic uncertainties for the coupling of the ALP to a photon pair and the branching fraction measurements include those from the number of signal events, the reconstruction efficiency, the total number of J/ψ events, and the branching fraction of $J/\psi \to e^+e^-$. The uncertainties associated with the number of signal events are additive because they originate from the PDF parameters of signal and backgrounds and the fit bias. The additive systematic uncertainty affects the significance of any observation and does not scale with the number of reconstructed signal events. We take into account the uncertainties associated with the PDF parameters of signal and backgrounds by performing the alternative fits at each m_a point using alternative PDFs, as described above. We utilize a large number of pseudoexperiments to test the reliability of the ML fit procedure and the accuracy of the signal and background modeling. The signal yields are extracted from these samples using the same fit method as described above. The biases are consistent with zero and their average uncertainty is 9.2 events, which is taken as an additional additive systematic uncertainty ($\sigma_{\rm add}$).

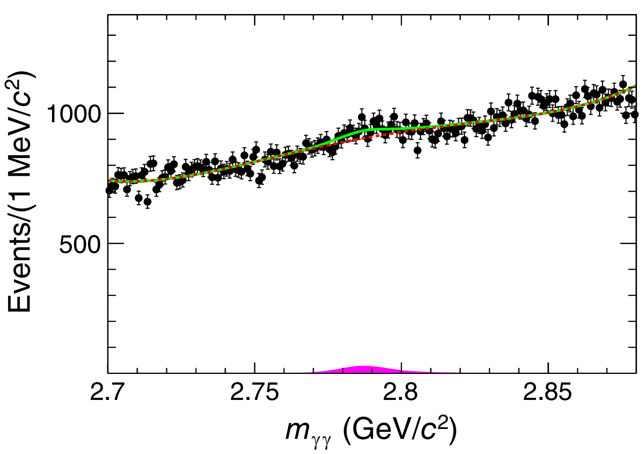

FIG. 3. Fit to the $m_{\gamma\gamma}$ distribution for $m_a = 2.786$ GeV$/c^2$. The black dots with error bars represent data, the dashed red curve is the continuum background, the filled pink curve is the signal PDF, and the solid green curve is the total fit result.

The other sources of the systematic uncertainties are multiplicative; they scale with the number of reconstructed events and do not affect the significance of a yield. The uncertainty associated with the reconstruction efficiency includes contributions from the 4C kinematic fit, the selection criteria of ΔE_{ij} and $\Delta\phi_{13}$, and the photon detection efficiency.

We use a control sample of $J/\psi \to \gamma\eta$, $\eta \to \gamma\gamma$ to evaluate the systematic uncertainties associated with the $\chi^2_{4\rm C}$, $\Delta E_{\gamma_{13}}$, $\Delta E_{\gamma_{23}}$, and $J/\psi \to \gamma P$ veto, and $\Delta\phi_{13}$ requirements. The signal yields for $J/\psi \to \gamma\eta$ from both data and MC simulation are extracted by performing an ML fit to the $m_{\gamma\gamma}$ distribution using the same fit procedure as described above. The corresponding systematic uncertainties, computed as the relative change in efficiency between data and MC simulation, are determined to be 2.3%, 0.1%, 0.1%, 0.8%, and 0.1%, respectively. The systematic uncertainty associated with the total number of J/ψ events is determined to be 0.44% with a sample of inclusive J/ψ hadronic events [43].

A control sample of $e^+e^- \to \gamma\mu^+\mu^-$ is used to evaluate the systematic uncertainty associated with the photon reconstruction efficiency. An ISR photon in this control sample is predicted using the four momenta of the two charged particles. This sample also includes the contributions from $e^+e^- \to \gamma\pi^+\pi^-$ and $J/\psi \to \gamma\pi^+\pi^-$, including all the possible intermediate resonances. The relative difference of efficiency between data and MC simulation is determined to be 0.2% per photon [60]. Thus, the total systematic uncertainty due to photon reconstruction efficiency for the three-photon candidates is 0.6%. The uncertainty associated with the branching fraction of $J/\psi \to e^+e^-$ is 0.5% taken from the PDG [46]. The total multiplicative systematic uncertainty ($\sigma_{\rm mult}$) is obtained by adding the individual ones in quadrature, and is determined to be 2.6% for both a product branching fraction $\mathcal{B}(J/\psi \to \gamma a) \times \mathcal{B}(a \to \gamma\gamma)$ and a coupling of ALP to a photon pair

TABLE II. The sources of systematic uncertainties. The uncertainties associated with the signal and background PDFs are incorporated into the fit, as described in the text.

Source	Uncertainty	
	$J/\psi \to \gamma a$	$g_{a\gamma\gamma}$ (GeV)$^{-1}$
Additive (events)		
Fit bias	9.2	9.2
Multiplicative (%)		
χ^2_{4C}	2.3	2.3
$\Delta E_{\gamma_{13}}$	0.1	0.1
$\Delta E_{\gamma_{23}}$	0.1	0.1
$J/\psi \to \gamma P$ veto	0.8	0.8
$\Delta\phi_{\gamma_{31}}$	0.1	0.1
$\mathcal{B}(J/\psi \to e^+e^-)$	…	0.5
J/ψ counting	0.44	0.44
Photon detection efficiency	0.6	0.6
Total	2.6	2.6

$g_{a\gamma\gamma}$. All sources of systematic uncertainties are summarized in Table II. We calculate the final systematic uncertainty as $\sqrt{\sigma^2_{\rm add} + (\sigma_{\rm mult} \times N_{\rm sig})^2}$.

Since no significant evidence of any signal events is found, we set the 95% confidence level (CL) upper limits on the product branching fraction $\mathcal{B}(J/\psi \to \gamma a) \times \mathcal{B}(a \to \gamma\gamma)$ as a function of m_a using a Bayesian approach with a uniform prior. The systematic uncertainty is included by convolving the likelihood function with a Gaussian function having a width equal to the systematic uncertainty.

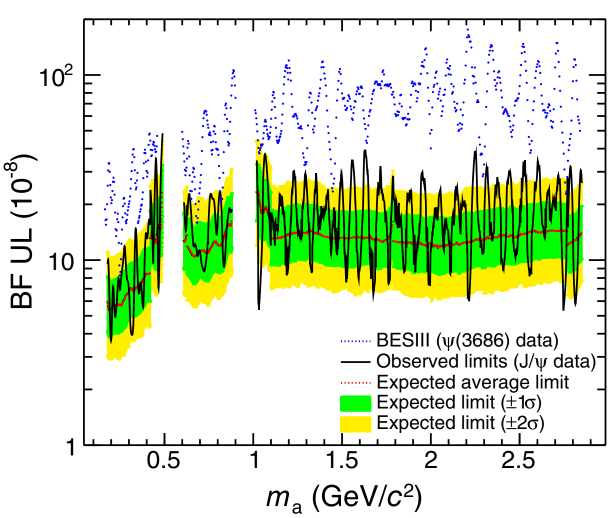

FIG. 4. Upper limits at the 95% CL on the product branching fraction $\mathcal{B}(J/\psi \to \gamma a) \times \mathcal{B}(a \to \gamma\gamma)$, including the systematic uncertainties, and compared with the previous BESIII measurements [42] as a function of m_a. The expected limit bands at $\pm 1\sigma$ and $\pm 2\sigma$ levels, obtained from a large ensemble of pseudoexperiments, include statistical uncertainty only.

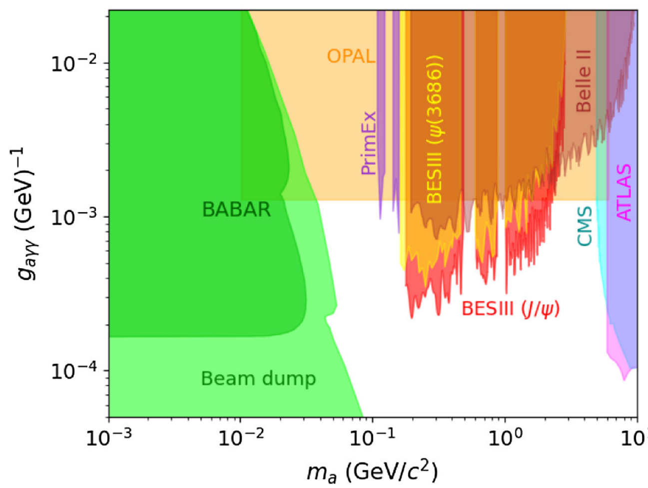

FIG. 5. The 95% CL upper limits on the coupling of ALP to a photon pair ($g_{a\gamma\gamma}$) together with *BABAR* [30], CMS [37], ATLAS [38], PrimEx [25], beam-dump [26,27], OPAL [34], previous BESIII [42], and Belle II [36] measurements as a function of m_a.

The limits range between 3.7×10^{-8} and 48.5×10^{-8} for $0.18 \le m_a \le 2.85$ GeV/c^2, as shown in Fig. 4 together with expected limit bands at $\pm 1\sigma$ and $\pm 2\sigma$ levels obtained from a large ensemble of pseudoexperiments. Our results improve upon the previous BESIII measurement [42] by an average factor of 8 to 9. Finally, we also calculate the 95% CL upper limit on $g_{a\gamma\gamma}$ using Eq. (1) while assuming $\mathcal{B}(a \to \gamma\gamma) = 1$ and including the additional sources of the systematic uncertainties on $\mathcal{B}(J/\psi \to e^+e^-)$ using a Bayesian approach with a uniform prior in a negative log-likelihood versus $g^2_{a\gamma\gamma}$ curve. The corresponding exclusion range is shown in Fig. 5. The limit varies within $(2.2\text{–}101.8) \times 10^{-4}$ (GeV)$^{-1}$ for $0.18 \le m_a \le 2.85$ GeV/c^2 and improves previous bounds set by previous BESIII [42] and Belle II [36] by factors of about 3 and 5, respectively. It has also twofold improvement over the OPAL measurement [34] for $1.468 \le m_a \le 2.2$ GeV/c^2.

In summary, we search for diphoton decays of a light pseudoscalar particle in radiative J/ψ decays, using $10^{10} J/\psi$ events collected by the BESIII detector. No significant evidence of signal events is found, and we set 95% CL upper limits on the product branching fraction $\mathcal{B}(J/\psi \to \gamma a) \times \mathcal{B}(a \to \gamma\gamma)$ and the coupling of the ALP to a photon pair $g_{a\gamma\gamma}$ as a function of m_a. The corresponding limits are more stringent than the existing limits from OPAL [34], previous BESIII [42], and Belle II [36] for $0.18 \le m_a \le 2.85$ GeV/c^2. These improved limits can significantly constrain the parameter spaces of the extended Higgs sector models [8,19,20,45] and other new physics models [5–7,14,22] in the investigated mass region.

The BESIII Collaboration thanks the staff of BEPCII and the IHEP computing center for their strong support. This work is supported in part by the National Key R&D

Program of China under Contracts No. 2020YFA0406300 and No. 2020YFA0406400; the National Natural Science Foundation of China (NSFC) under Contracts No. 11635010, No. 11735014, No. 11835012, No. 11935015, No. 11935016, No. 11935018, No. 11961141012, No. 12025502, No. 12035009, No. 12035013, No. 12061131003, No. 12192260, No. 12192261, No. 12192262, No. 12192263, No. 12192264, No. 12192265, No. 12221005, No. 12225509, No. 12235017, No. 11950410506, and No. 11705192; the Chinese Academy of Sciences (CAS) Large-Scale Scientific Facility Program; the CAS Center for Excellence in Particle Physics (CCEPP); Joint Large-Scale Scientific Facility Funds of the NSFC and CAS under Contract No. U1832207; the CAS Key Research Program of Frontier Sciences under Contracts No. QYZDJ-SSW-SLH003 and No. QYZDJ-SSW-SLH040; the 100 Talents Program of CAS; The Institute of Nuclear and Particle Physics (INPAC) and Shanghai Key Laboratory for Particle Physics and Cosmology; European Union's Horizon 2020 research and innovation program under Marie Skłodowska-Curie grant agreement under Contract No. 894790; the German Research Foundation (DFG) under Contracts No. 455635585, Collaborative Research Center No. CRC 1044, No. FOR5327, and No. GRK 2149; Istituto Nazionale di Fisica Nucleare, Italy; Ministry of Development of Turkey under Contract No. DPT2006K-120470; National Research Foundation of Korea under Contract No. NRF-2022R1A2C1092335; the National Science and Technology fund of Mongolia; National Science Research and Innovation Fund (NSRF) via the Program Management Unit for Human Resources and Institutional Development, Research and Innovation of Thailand under Contract No. B16F640076; Polish National Science Centre under Contract No. 2019/35/O/ST2/02907; The Chilean National Agency for Research and Development ANID PIA/APOYO AFB230003; and The Swedish Research Council; U.S. Department of Energy under Contract No. DE-FG02-05ER41374.

[1] R. D. Peccei and H. R. Quinn, Phys. Rev. Lett. **38**, 1440 (1977); Phys. Rev. D **16**, 1791 (1977).
[2] S. Weinberg, Phys. Rev. Lett. **40**, 223 (1978).
[3] F. Wilczek, Phys. Rev. Lett. **40**, 279 (1978).
[4] P. W. Graham, D. E. Kaplan, and S. Rajendran, Phys. Rev. Lett. **115**, 221801 (2015).
[5] J. Frere, D. Jones, and S. Raby, Nucl. Phys. **B222**, 11 (1983).
[6] A. E. Nelson and N. Seiberg, Nucl. Phys. **B416**, 46 (1994).
[7] J. Bagger, E. Poppitz, and L. Randall, Nucl. Phys. **B426**, 3 (1994).
[8] G. C. Branco, P. M. Ferreira, L. Lavoura, M. N. Rebelo, M. Sher, and J. P. Silva, Phys. Rep. **516**, 1 (2012).
[9] E. Witten, Phys. Lett. **149B**, 351 (1984).
[10] J. P. Conlon, J. High Energy Phys. 05 (2006) 078.
[11] P. Svrcek and E. Witten, J. High Energy Phys. 06 (2006) 051.
[12] A. Arvanitaki, S. Dimopoulos, S. Dubovsky, N. Kaloper, and J. March-Russell, Phys. Rev. D **81**, 123530 (2010).
[13] Y. Nomura and J. Thaler, Phys. Rev. D **79**, 075008 (2009).
[14] M. Freytsis and Z. Ligeti, Phys. Rev. D **83**, 115009 (2011).
[15] J. Preskill, M. B. Wise, and F. Wilczek, Phys. Lett. **120B**, 127 (1983).
[16] L. F. Abbott and P. Sikivie, Phys. Lett. **120B**, 133 (1983).
[17] M. Dine and W. Fischler, Phys. Lett. **120B**, 137 (1983).
[18] R. A. Battye, B. Garbrecht, J. I. McDonald, F. Pace, and S. Srinivasan, Phys. Rev. D **102**, 023504 (2020).
[19] S. Hesselbach, S. Moretti, S. Munir, and P. Poulose, Eur. Phys. J. C **54**, 129 (2008).
[20] A. Delgado, M. G. Pepin, M. Quiros, J. Santiago, and R. V. Morales, J. High Energy Phys. 06 (2016) 042.
[21] D. Curtin *et al.*, Phys. Rev. D **90**, 075004 (2014).
[22] D. D. Enterria, M. A. Tamlihat, L. Schoeffel, H.-S. Shao, and Y. Tayalati, Phys. Lett. B **846**, 138237 (2023).
[23] P. W. Graham *et al.*, Rev. Nucl. Part. Sci. **65**, 485 (2015).
[24] D. Cadamuro and J. Redondo, J. Cosmol. Astropart. Phys. 02 (2012) 032.
[25] D. Aloni, C. Fanelli, Y. Soreq, and M. Williams, Phys. Rev. Lett. **123**, 071801 (2019).
[26] B. Dobrich, J. Jaeckel, F. Kahlhoefer, A. Ringwald, and K. Schmidt-Hoberg, J. High Energy Phys. 02 (2016) 018.
[27] D. Banerjee *et al.* (NA64 Collaboration), Phys. Rev. Lett. **125**, 081801 (2020).
[28] M. Ablikim *et al.* (BESIII Collaboration), Phys. Rev. D **101**, 112005 (2020).
[29] I. S. Seong *et al.* (Belle Collaboration), Phys. Rev. Lett. **122**, 011801 (2019).
[30] M. J. Dolan, T. Ferber, C. Hearty, F. Kahlhoefer, and K. Schmidt-Hoberg, J. High Energy Phys. 12 (2017) 094; 03 (2021) 190(E).
[31] J. P. Lees *et al.* (*BABAR* Collaboration), Phys. Rev. Lett. **119**, 131804 (2017).
[32] B. Aubert *et al.* (*BABAR* Collaboration), arXiv:0808.0017.
[33] P. del Amo Sanchez *et al.* (*BABAR* Collaboration), Phys. Rev. Lett. **107**, 021804 (2011).
[34] S. Knapen, T. Lin, H. Keong Lou, and T. Melia, Phys. Rev. Lett. **118**, 171801 (2017); G. Abbiendi *et al.* (OPAL Collaboration), Eur. Phys. J. C **26**, 331 (2003).
[35] M. Acciarri *et al.* (L3 Collaboration), Phys. Lett. B **345**, 609 (1995).
[36] F. Abudinen *et al.* (Belle II Collaboration), Phys. Rev. Lett. **125**, 161806 (2020).
[37] A. M. Sirunyan *et al.* (CMS Collaboration), Phys. Lett. B **797**, 134826 (2019).

[38] G. Aad *et al.* (ATLAS Collaboration), J. High Energy Phys. 03 (2021) 243; 11 (2021) 50.
[39] D. d'Enterria, in *Proceedings of the Workshop on Feebly Interacting Particles*, 2021; [arXiv:2102.08971].
[40] G. Aad *et al.* (ATLAS Collaboration), Phys. Rev. Lett. **113**, 171801 (2014).
[41] G. Aad *et al.* (ATLAS Collaboration), Eur. Phys. J. C **76**, 210 (2016).
[42] M. Ablikim *et al.* (BESIII Collaboration), Phys. Lett. B **838**, 137698 (2023).
[43] M. Ablikim *et al.* (BESIII Collaboration), Chin. Phys. C **46**, 074001 (2022).
[44] J. Jaeckel and M. Spannowsky, Phys. Lett. B **753**, 482 (2016).
[45] L. Merlo, F. Pobbe, S. Rigolin, and O. Sumensari, J. High Energy Phys. 06 (2019) 091.
[46] R. L. Workman *et al.* (Particle Data Group), Prog. Theor. Exp. Phys. (2022) 083C01.
[47] M. Ablikim *et al.* (BESIII Collaboration), Phys. Rev. D **108**, 092002 (2023).
[48] M. Ablikim *et al.* (BESIII Collaboration), Nucl. Instrum. Methods Phys. Res., Sect. A **614**, 345 (2010); K. X. Huang *et al.*, Nucl. Sci. Technol. **33**, 142 (2022).
[49] C. H. Yu *et al.*, in *Proceedings of IPAC2016, Busan, Korea* (2016), edited by C. Petit-Jean-Genaz, D. E. Kim, K. S. Kim, I. S. Ko, and V. R. W. Schaa, 10.18429/JACoW-IPAC2016-TUYA01.
[50] M. Ablikim *et al.* (BESIII Collaboration), Chin. Phys. C **44**, 040001 (2020).
[51] J. Lu, Y. Xiao, and X. Ji, Radiat. Detect. Technol. Methods **4**, 337 (2020).
[52] J.-W. Zhang *et al.*, Radiat. Detect. Technol. Methods **6**, 289 (2022).
[53] S. Agostinelli *et al.* (GEANT4 Collaboration), Nucl. Instrum. Methods Phys. Res., Sect. A **506**, 250 (2003).
[54] X. Y. Zhou, S. X. Du, G. Li, and C. P. Shen, Comput. Phys. Commun. **258**, 107540 (2021).
[55] D. J. Lange, Nucl. Instrum. Methods Phys. Res., Sect. A **462**, 152 (2001); R. G. Ping, Chin. Phys. C **32**, 599 (2008).
[56] J. C. Chen, G. S. Huang, X. R. Qi, D. H. Zhang, and Y. S. Zhu, Phys. Rev. D **62**, 034003 (2000).
[57] S. Jadach, B. F. L. Ward, and Z. Was, Phys. Rev. D **63**, 113009 (2001).
[58] The Cruijff function is an asymmetric Gaussian function having a common mean (μ), different left-right resolutions ($\sigma_{L,R}$), and non-Gaussian tails ($\alpha_{L,R}$): $f(x) = \exp((x-\mu)^2/(2\sigma_{L,R}^2 + \alpha_{L,R}(x-\mu)^2))$.
[59] J. P. Lees *et al.* (*BABAR* Collaboration), Phys. Rev. D **87**, 059903(R) (2013); V. Prasad, Ph.D. thesis [Report No. SLAC-R-1008, 2013 (unpublished)]; arXiv:1307.4560, 2013.
[60] M. Ablikim *et al.* (BESIII Collaboration), Phys. Rev. D **105**, 012008 (2022).

M. Ablikim,[1] M. N. Achasov,[4,b] P. Adlarson,[75] X. C. Ai,[80] R. Aliberti,[35] A. Amoroso,[74a,74c] M. R. An,[39] Q. An,[71,58] Y. Bai,[57] O. Bakina,[36] I. Balossino,[29a] Y. Ban,[46,g] H.-R. Bao,[63] V. Batozskaya,[1,44] K. Begzsuren,[32] N. Berger,[35] M. Berlowski,[44] M. Bertani,[28a] D. Bettoni,[29a] F. Bianchi,[74a,74c] E. Bianco,[74a,74c] A. Bortone,[74a,74c] I. Boyko,[36] R. A. Briere,[5] A. Brueggemann,[68] H. Cai,[76] X. Cai,[1,58] A. Calcaterra,[28a] G. F. Cao,[1,63] N. Cao,[1,63] S. A. Cetin,[62a] J. F. Chang,[1,58] W. L. Chang,[1,63] G. R. Che,[43] G. Chelkov,[36,a] C. Chen,[43] Chao Chen,[55] G. Chen,[1] H. S. Chen,[1,63] M. L. Chen,[1,58,63] S. J. Chen,[42] S. L. Chen,[45] S. M. Chen,[61] T. Chen,[1,63] X. R. Chen,[31,63] X. T. Chen,[1,63] Y. B. Chen,[1,58] Y. Q. Chen,[34] Z. J. Chen,[25,h] S. K. Choi,[10] X. Chu,[43] G. Cibinetto,[29a] S. C. Coen,[3] F. Cossio,[74c] J. J. Cui,[50] H. L. Dai,[1,58] J. P. Dai,[78] A. Dbeyssi,[18] R. E. de Boer,[3] D. Dedovich,[36] Z. Y. Deng,[1] A. Denig,[35] I. Denysenko,[36] M. Destefanis,[74a,74c] F. De Mori,[74a,74c] B. Ding,[66,1] X. X. Ding,[46,g] Y. Ding,[34] Y. Ding,[40] J. Dong,[1,58] L. Y. Dong,[1,63] M. Y. Dong,[1,58,63] X. Dong,[76] M. C. Du,[1] S. X. Du,[80] Z. H. Duan,[42] P. Egorov,[36,a] Y. H. Fan,[45] J. Fang,[1,58] S. S. Fang,[1,63] W. X. Fang,[1] Y. Fang,[1] Y. Q. Fang,[1,58] R. Farinelli,[29a] L. Fava,[74b,74c] F. Feldbauer,[3] G. Felici,[28a] C. Q. Feng,[71,58] J. H. Feng,[59] Y. T. Feng,[71,58] K. Fischer,[69] M. Fritsch,[3] C. D. Fu,[1] J. L. Fu,[63] Y. W. Fu,[1] H. Gao,[63] Y. N. Gao,[46,g] Yang Gao,[71,58] S. Garbolino,[74c] I. Garzia,[29a,29b] P. T. Ge,[76] Z. W. Ge,[42] C. Geng,[59] E. M. Gersabeck,[67] A. Gilman,[69] K. Goetzen,[13] L. Gong,[40] W. X. Gong,[1,58] W. Gradl,[35] S. Gramigna,[29a,29b] M. Greco,[74a,74c] M. H. Gu,[1,58] Y. T. Gu,[15] C. Y. Guan,[1,63] Z. L. Guan,[22] A. Q. Guo,[31,63] L. B. Guo,[41] M. J. Guo,[50] R. P. Guo,[49] Y. P. Guo,[12,f] A. Guskov,[36,a] J. Gutierrez,[27] K. L. Han,[63] T. T. Han,[1] W. Y. Han,[39] X. Q. Hao,[19] F. A. Harris,[65] K. K. He,[55] K. L. He,[1,63] F. H. H. Heinsius,[3] C. H. Heinz,[35] Y. K. Heng,[1,58,63] C. Herold,[60] T. Holtmann,[3] P. C. Hong,[12,f] G. Y. Hou,[1,63] X. T. Hou,[1,63] Y. R. Hou,[63] Z. L. Hou,[1] B. Y. Hu,[59] H. M. Hu,[1,63] J. F. Hu,[56,i] T. Hu,[1,58,63] Y. Hu,[1] G. S. Huang,[71,58] K. X. Huang,[59] L. Q. Huang,[31,63] X. T. Huang,[50] Y. P. Huang,[1] T. Hussain,[73] N. Hüsken,[27,35] N. in der Wiesche,[68] M. Irshad,[71,58] J. Jackson,[27] S. Jaeger,[3] S. Janchiv,[32] J. H. Jeong,[10] Q. Ji,[1] Q. P. Ji,[19] X. B. Ji,[1,63] X. L. Ji,[1,58] Y. Y. Ji,[50] X. Q. Jia,[50] Z. K. Jia,[71,58] H. B. Jiang,[76] P. C. Jiang,[46,g] S. S. Jiang,[39] T. J. Jiang,[16] X. S. Jiang,[1,58,63] Y. Jiang,[63] J. B. Jiao,[50] Z. Jiao,[23] S. Jin,[42] Y. Jin,[66] M. Q. Jing,[1,63] X. M. Jing,[63] T. Johansson,[75] K. X. Huang,[1] S. Kabana,[33] N. Kalantar-Nayestanaki,[64] X. L. Kang,[9] X. S. Kang,[40] M. Kavatsyuk,[64] B. C. Ke,[80] V. Khachatryan,[27] A. Khoukaz,[68] R. Kiuchi,[1] O. B. Kolcu,[62a] B. Kopf,[3] M. Kuessner,[3] A. Kupsc,[44,75] W. Kühn,[37] J. J. Lane,[67] P. Larin,[18] L. Lavezzi,[74a,74c] T. T. Lei,[71,58] Z. H. Lei,[71,58] H. Leithoff,[35] M. Lellmann,[35] T. Lenz,[35] C. Li,[43] C. Li,[47] C. H. Li,[39] Cheng Li,[71,58] D. M. Li,[80]

F. Li,[1,58] G. Li,[1] H. Li,[71,58] H. B. Li,[1,63] H. J. Li,[19] H. N. Li,[56,i] Hui Li,[43] J. R. Li,[61] J. S. Li,[59] J. W. Li,[50] Ke Li,[1] L. J. Li,[1,63] L. K. Li,[1] Lei Li,[48] M. H. Li,[43] P. R. Li,[38,k] Q. X. Li,[50] S. X. Li,[12] T. Li,[50] W. D. Li,[1,63] W. G. Li,[1] X. H. Li,[71,58] X. L. Li,[50] Xiaoyu Li,[1,63] Y. G. Li,[46,g] Z. J. Li,[59] Z. X. Li,[15] C. Liang,[42] H. Liang,[71,58] H. Liang,[1,63] Y. F. Liang,[54] Y. T. Liang,[31,63] G. R. Liao,[14] L. Z. Liao,[50] Y. P. Liao,[1,63] J. Libby,[26] A. Limphirat,[60] D. X. Lin,[31,63] T. Lin,[1] B. J. Liu,[1] B. X. Liu,[76] C. Liu,[34] C. X. Liu,[1] F. H. Liu,[53] Fang Liu,[1] Feng Liu,[6] G. M. Liu,[56,i] H. Liu,[38,j,k] H. B. Liu,[15] H. M. Liu,[1,63] Huanhuan Liu,[1] Huihui Liu,[21] J. B. Liu,[71,58] J. Y. Liu,[1,63] K. Liu,[38,j,k] K. Y. Liu,[40] Ke Liu,[22] L. Liu,[71,58] L. C. Liu,[43] Lu Liu,[43] M. H. Liu,[12,f] P. L. Liu,[1] Q. Liu,[63] S. B. Liu,[71,58] T. Liu,[12,f] W. K. Liu,[43] W. M. Liu,[71,58] X. Liu,[38,j,k] Y. Liu,[38,j,k] Y. Liu,[80] Y. B. Liu,[43] Z. A. Liu,[1,58,63] Z. Q. Liu,[50] X. C. Lou,[1,58,63] F. X. Lu,[59] H. J. Lu,[23] J. G. Lu,[1,58] X. L. Lu,[1] Y. Lu,[7] Y. P. Lu,[1,58] Z. H. Lu,[1,63] C. L. Luo,[41] M. X. Luo,[79] T. Luo,[12,f] X. L. Luo,[1,58] X. R. Lyu,[63] Y. F. Lyu,[43] F. C. Ma,[40] H. Ma,[78] H. L. Ma,[1] J. L. Ma,[1,63] L. L. Ma,[50] M. M. Ma,[1,63] Q. M. Ma,[1] R. Q. Ma,[1,63] X. Y. Ma,[1,58] Y. Ma,[46,g] Y. M. Ma,[31] F. E. Maas,[18] M. Maggiora,[74a,74c] S. Malde,[69] A. Mangoni,[28b] Y. J. Mao,[46,g] Z. P. Mao,[1] S. Marcello,[74a,74c] Z. X. Meng,[66] J. G. Messchendorp,[13,64] G. Mezzadri,[29a] H. Miao,[1,63] T. J. Min,[42] R. E. Mitchell,[27] X. H. Mo,[1,58,63] B. Moses,[27] N. Yu. Muchnoi,[4,b] J. Muskalla,[35] Y. Nefedov,[36] F. Nerling,[18,d] I. B. Nikolaev,[4,b] Z. Ning,[1,58] S. Nisar,[11,l] Q. L. Niu,[38,j,k] W. D. Niu,[55] Y. Niu,[50] S. L. Olsen,[63] Q. Ouyang,[1,58,63] S. Pacetti,[28b,28c] X. Pan,[55] Y. Pan,[57] A. Pathak,[34] P. Patteri,[28a] Y. P. Pei,[71,58] M. Pelizaeus,[3] H. P. Peng,[71,58] Y. Y. Peng,[38,j,k] K. Peters,[13,d] J. L. Ping,[41] R. G. Ping,[1,63] S. Plura,[35] V. Prasad,[33] F. Z. Qi,[1] H. Qi,[71,58] H. R. Qi,[61] M. Qi,[42] T. Y. Qi,[12,f] S. Qian,[1,58] W. B. Qian,[63] C. F. Qiao,[63] J. J. Qin,[72] L. Q. Qin,[14] X. S. Qin,[50] Z. H. Qin,[1,58] J. F. Qiu,[1] S. Q. Qu,[61] C. F. Redmer,[35] K. J. Ren,[39] A. Rivetti,[74c] M. Rolo,[74c] G. Rong,[1,63] Ch. Rosner,[18] S. N. Ruan,[43] N. Salone,[44] A. Sarantsev,[36,c] Y. Schelhaas,[35] K. Schoenning,[75] M. Scodeggio,[29a,29b] K. Y. Shan,[12,f] W. Shan,[24] X. Y. Shan,[71,58] J. F. Shangguan,[55] L. G. Shao,[1,63] M. Shao,[71,58] C. P. Shen,[12,f] H. F. Shen,[1,63] W. H. Shen,[63] X. Y. Shen,[1,63] B. A. Shi,[63] H. C. Shi,[71,58] J. L. Shi,[12] J. Y. Shi,[1] Q. Q. Shi,[55] R. S. Shi,[1,63] X. Shi,[1,58] J. J. Song,[19] T. Z. Song,[59] W. M. Song,[34,1] Y. J. Song,[12] S. Sosio,[74a,74c] S. Spataro,[74a,74c] F. Stieler,[35] Y. J. Su,[63] G. B. Sun,[76] G. X. Sun,[1] H. Sun,[63] H. K. Sun,[1] J. F. Sun,[19] K. Sun,[61] L. Sun,[76] S. S. Sun,[1,63] T. Sun,[51,e] W. Y. Sun,[34] Y. Sun,[9] Y. J. Sun,[71,58] Y. Z. Sun,[1] Z. T. Sun,[50] Y. X. Tan,[71,58] C. J. Tang,[54] G. Y. Tang,[1] J. Tang,[59] Y. A. Tang,[76] L. Y. Tao,[72] Q. T. Tao,[25,h] M. Tat,[69] J. X. Teng,[71,58] V. Thoren,[75] W. H. Tian,[52] W. H. Tian,[59] Y. Tian,[31,63] Z. F. Tian,[76] I. Uman,[62b] Y. Wan,[55] S. J. Wang,[50] B. Wang,[1] B. L. Wang,[63] Bo Wang,[71,58] C. W. Wang,[42] D. Y. Wang,[46,g] F. Wang,[72] H. J. Wang,[38,j,k] J. P. Wang,[50] K. Wang,[1,58] L. L. Wang,[1] M. Wang,[50] Meng Wang,[1,63] N. Y. Wang,[63] S. Wang,[12,f] S. Wang,[38,j,k] T. Wang,[12,f] T. J. Wang,[43] W. Wang,[59] W. Wang,[72] W. P. Wang,[71,58] X. Wang,[46,g] X. F. Wang,[38,j,k] X. J. Wang,[39] X. L. Wang,[12,f] Y. Wang,[61] Y. D. Wang,[45] Y. F. Wang,[1,58,63] Y. L. Wang,[19] Y. N. Wang,[45] Y. Q. Wang,[1] Yaqian Wang,[17,1] Yi Wang,[61] Z. Wang,[1,58] Z. L. Wang,[72] Z. Y. Wang,[1,63] Ziyi Wang,[63] D. Wei,[70] D. H. Wei,[14] F. Weidner,[68] S. P. Wen,[1] C. W. Wenzel,[3] U. Wiedner,[3] G. Wilkinson,[69] M. Wolke,[75] L. Wollenberg,[3] C. Wu,[39] J. F. Wu,[1,8] L. H. Wu,[1] L. J. Wu,[1,63] X. Wu,[12,f] X. H. Wu,[34] Y. Wu,[71] Y. H. Wu,[55] Y. J. Wu,[31] Z. Wu,[1,58] L. Xia,[71,58] X. M. Xian,[39] T. Xiang,[46,g] D. Xiao,[38,j,k] G. Y. Xiao,[42] S. Y. Xiao,[1] Y. L. Xiao,[12,f] Z. J. Xiao,[41] C. Xie,[42] X. H. Xie,[46,g] Y. Xie,[50] Y. G. Xie,[1,58] Y. H. Xie,[6] Z. P. Xie,[71,58] T. Y. Xing,[1,63] C. F. Xu,[1,63] C. J. Xu,[59] G. F. Xu,[1] H. Y. Xu,[66] Q. J. Xu,[16] Q. N. Xu,[30] W. Xu,[1] W. L. Xu,[66] X. P. Xu,[55] Y. C. Xu,[77] Z. P. Xu,[42] Z. S. Xu,[63] F. Yan,[12,f] L. Yan,[12,f] W. B. Yan,[71,58] W. C. Yan,[80] X. Q. Yan,[1] H. J. Yang,[51,e] H. L. Yang,[34] H. X. Yang,[1] Tao Yang,[1] Y. Yang,[12,f] Y. F. Yang,[43] Y. X. Yang,[1,63] Yifan Yang,[1,63] Z. W. Yang,[38,j,k] Z. P. Yao,[50] M. Ye,[1,58] M. H. Ye,[8] J. H. Yin,[1] Z. Y. You,[59] B. X. Yu,[1,58,63] C. X. Yu,[43] G. Yu,[1,63] J. S. Yu,[25,h] T. Yu,[72] X. D. Yu,[46,g] C. Z. Yuan,[1,63] L. Yuan,[2] S. C. Yuan,[1] Y. Yuan,[1,63] Z. Y. Yuan,[59] C. X. Yue,[39] A. A. Zafar,[73] F. R. Zeng,[50] S. H. Zeng,[72] X. Zeng,[12,f] Y. Zeng,[25,h] Y. J. Zeng,[1,63] X. Y. Zhai,[34] Y. C. Zhai,[50] Y. H. Zhan,[59] A. Q. Zhang,[1,63] B. L. Zhang,[1,63] B. X. Zhang,[1] D. H. Zhang,[43] G. Y. Zhang,[19] H. Zhang,[71] H. C. Zhang,[1,58,63] H. H. Zhang,[59] H. H. Zhang,[34] H. Q. Zhang,[1,58,63] H. Y. Zhang,[1,58] J. Zhang,[80] J. Zhang,[59] J. J. Zhang,[52] J. L. Zhang,[20] J. Q. Zhang,[41] J. W. Zhang,[1,58,63] J. X. Zhang,[38,j,k] J. Y. Zhang,[1] J. Z. Zhang,[1,63] Jianyu Zhang,[63] L. M. Zhang,[61] L. Q. Zhang,[59] Lei Zhang,[42] P. Zhang,[1,63] Q. Y. Zhang,[39,80] Shuihan Zhang,[1,63] Shulei Zhang,[25,h] X. D. Zhang,[45] X. M. Zhang,[1] X. Y. Zhang,[50] Y. Zhang,[69] Y. Zhang,[72] Y. T. Zhang,[80] Y. H. Zhang,[1,58] Yan Zhang,[71,58] Yao Zhang,[1] Z. D. Zhang,[1] Z. H. Zhang,[1] Z. L. Zhang,[34] Z. Y. Zhang,[43] Z. Y. Zhang,[76] G. Zhao,[1] J. Y. Zhao,[1,63] J. Z. Zhao,[1,58] Lei Zhao,[71,58] Ling Zhao,[1] M. G. Zhao,[43] R. P. Zhao,[63] S. J. Zhao,[80] Y. B. Zhao,[1,58] Y. X. Zhao,[31,63] Z. G. Zhao,[71,58] A. Zhemchugov,[36,a] B. Zheng,[72] J. P. Zheng,[1,58] W. J. Zheng,[1,63] Y. H. Zheng,[63] B. Zhong,[41] X. Zhong,[59] H. Zhou,[50] L. P. Zhou,[1,63] X. Zhou,[76] X. K. Zhou,[6] X. R. Zhou,[71,58] X. Y. Zhou,[39] Y. Z. Zhou,[12,f] J. Zhu,[43] K. Zhu,[1] K. J. Zhu,[1,58,63] L. Zhu,[34] L. X. Zhu,[63] S. H. Zhu,[70] S. Q. Zhu,[42] T. J. Zhu,[12,f] W. J. Zhu,[12,f] Y. C. Zhu,[71,58] Z. A. Zhu,[1,63] J. H. Zou,[1] and J. Zu[71,58]

(BESIII Collaboration)

[1]*Institute of High Energy Physics, Beijing 100049, People's Republic of China*
[2]*Beihang University, Beijing 100191, People's Republic of China*
[3]*Bochum Ruhr-University, D-44780 Bochum, Germany*
[4]*Budker Institute of Nuclear Physics SB RAS (BINP), Novosibirsk 630090, Russia*
[5]*Carnegie Mellon University, Pittsburgh, Pennsylvania 15213, USA*
[6]*Central China Normal University, Wuhan 430079, People's Republic of China*
[7]*Central South University, Changsha 410083, People's Republic of China*
[8]*China Center of Advanced Science and Technology, Beijing 100190, People's Republic of China*
[9]*China University of Geosciences, Wuhan 430074, People's Republic of China*
[10]*Chung-Ang University, Seoul 06974, Republic of Korea*
[11]*COMSATS University Islamabad, Lahore Campus, Defence Road, Off Raiwind Road, 54000 Lahore, Pakistan*
[12]*Fudan University, Shanghai 200433, People's Republic of China*
[13]*GSI Helmholtzcentre for Heavy Ion Research GmbH, D-64291 Darmstadt, Germany*
[14]*Guangxi Normal University, Guilin 541004, People's Republic of China*
[15]*Guangxi University, Nanning 530004, People's Republic of China*
[16]*Hangzhou Normal University, Hangzhou 310036, People's Republic of China*
[17]*Hebei University, Baoding 071002, People's Republic of China*
[18]*Helmholtz Institute Mainz, Staudinger Weg 18, D-55099 Mainz, Germany*
[19]*Henan Normal University, Xinxiang 453007, People's Republic of China*
[20]*Henan University, Kaifeng 475004, People's Republic of China*
[21]*Henan University of Science and Technology, Luoyang 471003, People's Republic of China*
[22]*Henan University of Technology, Zhengzhou 450001, People's Republic of China*
[23]*Huangshan College, Huangshan 245000, People's Republic of China*
[24]*Hunan Normal University, Changsha 410081, People's Republic of China*
[25]*Hunan University, Changsha 410082, People's Republic of China*
[26]*Indian Institute of Technology Madras, Chennai 600036, India*
[27]*Indiana University, Bloomington, Indiana 47405, USA*
[28a]*INFN Laboratori Nazionali di Frascati, I-00044 Frascati, Italy*
[28b]*INFN Sezione di Perugia, I-06100 Perugia, Italy*
[28c]*University of Perugia, I-06100 Perugia, Italy*
[29a]*INFN Sezione di Ferrara, I-44122 Ferrara, Italy*
[29b]*University of Ferrara, I-44122 Ferrara, Italy*
[30]*Inner Mongolia University, Hohhot 010021, People's Republic of China*
[31]*Institute of Modern Physics, Lanzhou 730000, People's Republic of China*
[32]*Institute of Physics and Technology, Peace Avenue 54B, Ulaanbaatar 13330, Mongolia*
[33]*Instituto de Alta Investigación, Universidad de Tarapacá, Casilla 7D, Arica 1000000, Chile*
[34]*Jilin University, Changchun 130012, People's Republic of China*
[35]*Johannes Gutenberg University of Mainz, Johann-Joachim-Becher-Weg 45, D-55099 Mainz, Germany*
[36]*Joint Institute for Nuclear Research, 141980 Dubna, Moscow Region, Russia*
[37]*Justus-Liebig-Universitaet Giessen, II. Physikalisches Institut, Heinrich-Buff-Ring 16, D-35392 Giessen, Germany*
[38]*Lanzhou University, Lanzhou 730000, People's Republic of China*
[39]*Liaoning Normal University, Dalian 116029, People's Republic of China*
[40]*Liaoning University, Shenyang 110036, People's Republic of China*
[41]*Nanjing Normal University, Nanjing 210023, People's Republic of China*
[42]*Nanjing University, Nanjing 210093, People's Republic of China*
[43]*Nankai University, Tianjin 300071, People's Republic of China*
[44]*National Centre for Nuclear Research, Warsaw 02-093, Poland*
[45]*North China Electric Power University, Beijing 102206, People's Republic of China*
[46]*Peking University, Beijing 100871, People's Republic of China*
[47]*Qufu Normal University, Qufu 273165, People's Republic of China*
[48]*Renmin University of China, Beijing 100872, People's Republic of China*
[49]*Shandong Normal University, Jinan 250014, People's Republic of China*
[50]*Shandong University, Jinan 250100, People's Republic of China*
[51]*Shanghai Jiao Tong University, Shanghai 200240, People's Republic of China*
[52]*Shanxi Normal University, Linfen 041004, People's Republic of China*
[53]*Shanxi University, Taiyuan 030006, People's Republic of China*
[54]*Sichuan University, Chengdu 610064, People's Republic of China*

[55]*Soochow University, Suzhou 215006, People's Republic of China*
[56]*South China Normal University, Guangzhou 510006, People's Republic of China*
[57]*Southeast University, Nanjing 211100, People's Republic of China*
[58]*State Key Laboratory of Particle Detection and Electronics, Beijing 100049, Hefei 230026, People's Republic of China*
[59]*Sun Yat-Sen University, Guangzhou 510275, People's Republic of China*
[60]*Suranaree University of Technology, University Avenue 111, Nakhon Ratchasima 30000, Thailand*
[61]*Tsinghua University, Beijing 100084, People's Republic of China*
[62a]*Turkish Accelerator Center Particle Factory Group, Istinye University, 34010 Istanbul, Turkey*
[62b]*Near East University, Nicosia, North Cyprus 99138, Mersin 10, Turkey*
[63]*University of Chinese Academy of Sciences, Beijing 100049, People's Republic of China*
[64]*University of Groningen, NL-9747 AA Groningen, The Netherlands*
[65]*University of Hawaii, Honolulu, Hawaii 96822, USA*
[66]*University of Jinan, Jinan 250022, People's Republic of China*
[67]*University of Manchester, Oxford Road, Manchester M13 9PL, United Kingdom*
[68]*University of Muenster, Wilhelm-Klemm-Strasse 9, 48149 Muenster, Germany*
[69]*University of Oxford, Keble Road, Oxford OX13RH, United Kingdom*
[70]*University of Science and Technology Liaoning, Anshan 114051, People's Republic of China*
[71]*University of Science and Technology of China, Hefei 230026, People's Republic of China*
[72]*University of South China, Hengyang 421001, People's Republic of China*
[73]*University of the Punjab, Lahore-54590, Pakistan*
[74a]*University of Turin, I-10125 Turin, Italy*
[74b]*University of Eastern Piedmont, I-15121 Alessandria, Italy*
[74c]*INFN, I-10125 Turin, Italy*
[75]*Uppsala University, Box 516, SE-75120 Uppsala, Sweden*
[76]*Wuhan University, Wuhan 430072, People's Republic of China*
[77]*Yantai University, Yantai 264005, People's Republic of China*
[78]*Yunnan University, Kunming 650500, People's Republic of China*
[79]*Zhejiang University, Hangzhou 310027, People's Republic of China*
[80]*Zhengzhou University, Zhengzhou 450001, People's Republic of China*

[a]Also at the Moscow Institute of Physics and Technology, Moscow 141700, Russia.
[b]Also at the Novosibirsk State University, Novosibirsk 630090, Russia.
[c]Also at the NRC "Kurchatov Institute," PNPI, 188300 Gatchina, Russia.
[d]Also at Goethe University Frankfurt, 60323 Frankfurt am Main, Germany.
[e]Also at Key Laboratory for Particle Physics, Astrophysics and Cosmology, Ministry of Education; Shanghai Key Laboratory for Particle Physics and Cosmology; Institute of Nuclear and Particle Physics, Shanghai 200240, People's Republic of China.
[f]Also at Key Laboratory of Nuclear Physics and Ion-beam Application (MOE) and Institute of Modern Physics, Fudan University, Shanghai 200443, People's Republic of China.
[g]Also at State Key Laboratory of Nuclear Physics and Technology, Peking University, Beijing 100871, People's Republic of China.
[h]Also at School of Physics and Electronics, Hunan University, Changsha 410082, China.
[i]Also at Guangdong Provincial Key Laboratory of Nuclear Science, Institute of Quantum Matter, South China Normal University, Guangzhou 510006, China.
[j]Also at MOE Frontiers Science Center for Rare Isotopes, Lanzhou University, Lanzhou 730000, People's Republic of China.
[k]Also at Lanzhou Center for Theoretical Physics, Lanzhou University, Lanzhou 730000, People's Republic of China.
[l]Also at the Department of Mathematical Sciences, IBA, Karachi 75270, Pakistan.